

**Energetics of high-energy cosmic radiations**

Kohta Murase

*Department of Physics; Department of Astronomy & Astrophysics;  
Center for Particle and Gravitational Astrophysics, Pennsylvania State University,  
University Park, Pennsylvania 16802, USA  
and Yukawa Institute for Theoretical Physics, Kyoto University, Kyoto, Kyoto 606-8502, Japan*

Masataka Fukugita

*Institute for Advanced Study, Princeton, New Jersey 08540, USA  
and Kavli Institute for the Physics and Mathematics of the Universe,  
University of Tokyo, Kashiwa 277 8583, Japan*



(Received 11 June 2018; published 18 March 2019)

The luminosity densities of high-energy cosmic radiations are studied to find connections among the various components, including high-energy neutrinos measured with IceCube and gamma rays with the *Fermi* satellite. Matching the cosmic-ray energy generation rate density in a GeV–TeV range estimated for Milky Way with the ultra-high-energy component requires a power-law index of the spectrum  $s_{\text{cr}} \approx 2.1\text{--}2.2$ , somewhat harder than  $s_{\text{cr}} \approx 2.3\text{--}2.4$  for the local index derived from the AMS-02 experiment. The soft GeV–TeV cosmic-ray spectrum extrapolated to higher energies can be compatible with PeV cosmic rays inferred from neutrino measurements, but overshoots the CR luminosity density to explain GeV–TeV gamma rays. The extrapolation from ultrahigh energies with a hard spectrum, on the other hand, can be consistent with both neutrinos and gamma rays. These point towards either reacceleration of galactic cosmic rays or the presence of extragalactic sources with a hard spectrum. We discuss possible cosmic-ray sources that can be added.

DOI: [10.1103/PhysRevD.99.063012](https://doi.org/10.1103/PhysRevD.99.063012)**I. INTRODUCTION**

Cosmic rays (CRs) carry the energy about 1 eV per cubic centimetre in the solar neighborhood. This amounts to  $\Omega_{\text{cr}} \sim 10^{-11.4}$  when the local energy density is extended to the entire Milky Way galaxy and integrated over the optical luminosity function of galaxies, assuming that the CR energy is proportional to optical luminosity of galaxies [1]. It is known, however, that CRs leak from our Galaxy in a time scale about  $\sim 10\text{--}100$  Myr. When this is taken into account, assuming that leaked CRs survive without significant energy losses, the global CR energy density amounts to  $\Omega_{\text{cr}} \sim 10^{-8.3}$  [1]. This energy that represents the CR generation is about 20% of the cumulative amount of kinetic energies produced in core-collapse supernovae (ccSNe) integrated to higher redshifts,  $\Omega_{\text{sn,ke}} \sim 10^{-7.3}$  [1]. Such an energetics consideration endorses that the production of CRs is associated with the star-formation activity in galaxies.

In recent years, much information relevant to extragalactic CRs became available at very high energies. This would raise the question as to connections among various extragalactic cosmic particles and CRs that are locally observed [2,3]. The observations of high-energy CRs are supplemented by unprecedentedly accurate knowledge of

local CRs in the GeV–TeV region by PAMELA [4] and by AMS-02 [5], which leads us to infer accurately the propagation of Galactic CRs, and thus would in turn make clear the position of Galactic and extragalactic CRs in the universe.

Ultrahigh-energy (UHE) CRs in excess of  $10^{18.5}$  eV are likely to be extragalactic: further to the fact that they cannot be confined in the Galaxy, their spectrum shows a sharp decrease above the energy  $5 \times 10^{19}$  eV, as observed in the Pierre Auger Observatory [6] and the Telescope Array [7], which can be ascribed to the Greisen-Zatsepin-Kuzmin (GZK) and photodisintegration cutoffs, and indicates the origin of UHE CRs at a great distance of several tens of Mpc.

In addition, observations have been made for GeV–TeV gamma rays with the *Fermi* telescope (e.g., [8]), and for TeV–PeV cosmic neutrinos with the IceCube experiment (e.g., [9]). These experiments tell us about the high-energy CRs as primaries to be compared with the direct CR observation at lower energies.

In this paper, we focus on luminosity densities of GeV–TeV and UHE CRs, and those needed to account for high-energy gamma-ray and neutrino observations. We study physical connections among these components. This consideration hints us to clarify the origin of high-energy

cosmic particles. We consider that a typical error of our argument is no greater than 0.3 dex, unless otherwise explicitly noted, from a number of cross checks we have performed.

We take  $H_0 = 70 \text{ km s}^{-1} \text{ Mpc}^{-1}$ ,  $\Omega_m = 0.3$  and  $\Omega_\Lambda = 0.7$  for cosmological parameters.

## II. ENERGETICS OF COSMIC RADIATIONS

### A. Galactic cosmic rays

#### 1. Galactic cosmic-ray luminosity

The CR proton flux derived by AMS-02 is given approximately as [5]

$$E^2 \Phi_{\text{cr}} = 1.8 \times 10^{-2} \text{ GeV cm}^{-2} \text{ s}^{-1} \text{ sr}^{-1} \left( \frac{E}{300 \text{ GeV}} \right)^{2-\gamma_{\text{cr}}}, \quad (1)$$

for the kinetic energy  $E \gtrsim 50 \text{ GeV}$ , where  $\gamma_{\text{cr}}$  is the spectral index of CRs observed on Earth:  $\gamma_{\text{cr}} \approx 2.85$  below  $\sim 300 \text{ GeV}$  hardens to  $\gamma_{\text{cr}} \approx 2.72$  above  $\sim 300 \text{ GeV}$ . This hardening has been known from the CREAM [10] and PAMELA experiments [4]. The helium flux is known to be harder by  $\Delta\gamma_{\text{cr}} = -0.08$ , corresponding to  $\gamma_{\text{cr}} \approx 2.78$  below  $\sim 250 \text{ GeV}$  that hardens to  $\gamma_{\text{cr}} \approx 2.66$  above  $\sim 250 \text{ GeV}$  [11]. We use Refs. [5,11] for proton and helium fluxes above 46 GeV. For lower energies, where the solar modulation is more important, we adopt Ref. [12] that considers the latest Voyager data [13]. See also Ref. [14] for a detailed study on solar modulation effects.

The Galactic CR energy density is written

$$E dU_{\text{cr}}/dE = dU_{\text{cr}}/d \ln E = 4\pi E^2 \Phi_{\text{cr}}/v, \quad (2)$$

where  $v$  is the particle velocity. The total energy density of CR protons and helium nuclei is estimated to be  $U_{\text{cr}} = \int dE (dU_{\text{cr}}/dE) \approx 1 \text{ eV cm}^{-3}$ , consistent with the value based on Ref. [15], taking account of the solar modulation using the Fisk model with the solar potential 700 MV.

To evaluate the high-energy CR luminosity of the Milky Way, we take account of the fact that CRs eventually escape from the Galactic disc and the larger CR halo region. We here introduce the grammage along the CR path length  $X_{\text{esc}} \equiv \int dl n(l) \mu$ , where  $n(l)$  is the nucleon density and  $\mu \approx 1.4 m_p$  is the mean mass of gas. In the steady state,  $X_{\text{esc}}$  is related to the CR residence time  $t_{\text{esc}}$ , as  $X_{\text{esc}}(R) = \bar{n} \mu v t_{\text{esc}}(R)$ , where  $\bar{n}$  is the mean nucleon density in the CR confinement volume in the Milky Way. The CR halo, which is typically  $h \sim 1\text{--}10 \text{ kpc}$ , is larger than the scale height of the Galactic disc ( $\sim 300 \text{ pc}$ ). Correspondingly,  $\bar{n}$  should be lower than the averaged density in the Galactic disc, while the exact value is uncertain as it depends on the CR halo size [1] that is uncertain too. Instead, the grammage that

consists of the product of  $\bar{n}$  and  $t_{\text{esc}}$  can be determined better by CR data [16]. From the ratio of boron to carbon fluxes [17,18] the grammage (e.g., [16,19]) traversed by CRs is estimated to be

$$X_{\text{esc}}(R) \approx 8.7 \text{ g cm}^{-2} \left( \frac{R}{10 \text{ GV}} \right)^{-\delta}, \quad (3)$$

where  $R = cp/Ze$  is the rigidity. Whereas a single power law with  $\delta = 0.4$  gives a reasonable fit (with 20% accuracy) to the grammage deduced from the boron-to-carbon ratio data for  $R > 5 \text{ GV}$  [16], the recent AMS-02 measurement indicates a lower value,  $\delta = 0.333 \pm 0.014(\text{fit}) \pm 0.005(\text{syst})$  above 65 GeV [18]. Noting that  $\delta$  appears decreasing as energy increases [20], we take a broken power law with  $\delta = 0.46$  for  $R < 250 \text{ GV}$  and  $\delta = 0.33$  for  $R \geq 250 \text{ GV}$ . The hardening of the CR spectrum is then translated to this flatter energy dependence of the grammage at a higher rigidity: with the index of the CR injection spectrum  $s_{\text{cr}} = \gamma_{\text{cr}} - \delta = 2.39$  (for the proton) and 2.33 (for the helium),  $\delta$  can give proper spectral indices of CRs for a wide range of the energy (see also Ref. [20]). Our conclusions are unchanged by the choice of  $\delta$  within the uncertainty. We remark that for  $R \lesssim 20 \text{ GV}$  the *Fermi* measurement of gamma rays from nearby molecular clouds gives different indices, e.g.,  $\gamma_{\text{cr}} \approx 2.9$  for  $R \gtrsim 10\text{--}20 \text{ GV}$  [21], implying a steeper high-energy CR spectrum.

Now let us estimate the CR luminosity of the Milky Way. In the steady state, the differential CR luminosity satisfies  $E(dL_{\text{cr}}/dE)t_{\text{esc}} = E(dU_{\text{cr}}/dE)\mathcal{V}_{\text{halo}}$ , where  $\mathcal{V}_{\text{halo}}$  is the halo volume. This can be rewritten  $E(dL_{\text{cr}}/dE)X_{\text{esc}} = E(dU_{\text{cr}}/dE)M_{\text{gas}}$ , where  $M_{\text{gas}}$  is the total gas mass contained in the CR halo. In general, the gas mass consists of  $M_{\text{gas}} = M_{\text{cold}} + M_{\text{warm/hot}}$ , where  $M_{\text{cold}}$  is the cold gas mass in the disc region. The so-called missing baryon problem [22] implies that the latter, i.e., warm or hot circumgalactic mass, is significant in a scale of the virial radius of the Milky Way, which is about 250 kpc. References [23–25] suggest  $M_{\text{warm/hot}} \approx (1\text{--}4) \times 10^8 M_\odot$  within 15 kpc and  $M_{\text{warm/hot}} \approx (2\text{--}3) \times 10^9 M_\odot$  within 50 kpc. Thus, we can safely ignore the circumgalactic gas mass in a scale of the CR halo with  $h \sim 1\text{--}10 \text{ kpc}$ . The stellar mass of the Milky Way is estimated  $M_* = 5.1 \times 10^{10} M_\odot$  (e.g., [26]). The cold gas mass (H I, He I and molecular gas) estimated from HIPASS and CO surveys,  $\Omega_{\text{gas}}/\Omega_* = 0.00078/0.0027 \approx 29\%$  [1], which is consistent with an estimate for the gas mass of the Milky Way within a factor of 2 (e.g., [27]). Taking these uncertainties into account, we take the gas mass fraction to be 15%–30% of the stellar mass:  $M_{\text{gas}} \approx M_{\text{cold}} = (0.75\text{--}1.5) \times 10^{10} M_\odot$ . For the steady state, the Galactic CR proton luminosity per logarithmic energy range is, using Eq. (3),

$$\begin{aligned}
E \frac{dL_{\text{cr}}}{dE} &= E \frac{dU_{\text{cr}}}{dE} \frac{v\mathcal{V}_{\text{halo}}}{t_{\text{esc}}(E)} \\
&= E \frac{dU_{\text{cr}}}{dE} \frac{vM_{\text{gas}}}{X_{\text{esc}}(E)} \\
&\simeq 1.5 \times 10^{40} \text{ erg s}^{-1} \left( \frac{M_{\text{gas}}}{10^{10} M_{\odot}} \right) \left( \frac{E}{10 \text{ GeV}} \right)^{2-s_{\text{cr}}}.
\end{aligned} \tag{4}$$

We note that the above quantity is the differential luminosity multiplied by the relevant energy, which should be smaller than the integrated luminosity,  $L_{\text{cr}} = \int dE (dL_{\text{cr}}/dE)$ . With the helium contribution, Eq. (4) leads to  $L_{\text{cr}} \simeq 8.5 \times 10^{40} \text{ erg s}^{-1}$ , consistent with the estimate in Ref. [28] within 20%.

We remark that the derived CR luminosity is based on local CRs in the solar neighborhood. Observations of gamma rays from nearby molecular clouds [21] give a result consistent with this. The CR density may be larger toward the Galactic center. If we assume that the CR production is proportional to the radio emission [29], the total density of CRs may be larger than our estimate by a factor of 2 [1]. The recent observations in GeV–TeV gamma rays suggest that the CR density is higher by a factor of 5 within 100 pc of the Galactic center [30], or by a factor of 2–4 within the 3 kpc region [31,32]. These mean that the CR luminosity enhancement is at most modest, only up to by a factor of 2 when averaged over the galaxy.

Indeed, if one invokes a propagation model such as GALPROP, in which an inhomogeneous distribution of CRs including the enhancement around the Galactic center, can be captured [31,32], one obtains  $E(dL_{\text{cr}}/dE) \simeq 1.3 \times 10^{40} \text{ erg s}^{-1}$  around 10 GeV [33]. Our result in Eq. (4), without taking account of the enhancement by the CR inhomogeneity, agrees with variants of estimates to within a factor of 2. This is an example that our estimate of the uncertainty in the CR luminosity, typically less than 0.3 dex, in fact, holds.

## 2. Consistency with traditional estimates

Let us note here the consistency between CR and acceleration in remnants of ccSNe. If we take the conventional ccSN rate,  $\rho_{\text{sn}} = 1/30 \text{ yr}^{-1}$  [34], we find the average CR luminosity generated in the Milky Way galaxy,

$$E \frac{dL_{\text{cr}}}{dE} \simeq 2.1 \times 10^{40} \text{ erg s}^{-1} \left( \frac{\epsilon_{\text{cr}} \mathcal{E}_{\text{sn}}}{10^{50} \text{ erg}} \right) \left( \frac{E}{10 \text{ GeV}} \right)^{-0.39}, \tag{5}$$

taking the CR spectrum from AMS-02, the kinetic energy of a ccSN  $\mathcal{E}_{\text{sn}} \sim 10^{51} \text{ erg}$ , and the energy fraction carried by CRs  $\epsilon_{\text{cr}} \sim 0.1$ . This is consistent with Eq. (4). Thus, ccSNe may well account for the entire CR luminosity with the energy fraction carried by CRs,  $\epsilon_{\text{cr}} \sim 10\%$ .

The abundance of the secondary nuclei, boron, lithium, and beryllium indicates  $t_{\text{esc}} \sim 15\text{--}100 \text{ Myr}$  [35,36]. In particular, measurements of the beryllium ratio lead to  $t_{\text{esc}} = 15 \pm 1.6 \text{ Myr}$  with the aid of the leaky box model: the diffusion model predicts a longer time scale,  $t_{\text{esc}} \sim 30\text{--}100 \text{ Myr}$ , which depends on the CR halo size,  $h$  [35]. This is also consistent with Ref. [37]. These are at least by three orders of magnitude longer than the crossing time,  $t_{\text{cross}} = h/c \simeq 13 \text{ kyr}(h/4 \text{ kpc})$ . This escape time means that a dominant part of generated CRs escape. Namely, the fraction of CRs that reside in galaxies is  $\sim t_{\text{esc}}/t_H$  times the generated CRs (where  $t_H = 1/H_0$  is the Hubble time). Under the assumption that the CR halo size is energy independent, the simple diffusion model (e.g., [35,38]) gives

$$t_{\text{esc}}(R) \sim 60 \text{ Myr}(c/v)(R/1 \text{ GV})^{-\delta}, \tag{6}$$

which is consistent with the diffusion constant at 1 GV,  $D(1 \text{ GV}) \sim 4 \times 10^{28} \text{ cm}^2 \text{ s}^{-1}$  for  $h = 4 \text{ kpc}$ . If we assume that CRs reside in the CR halo with the volume of  $\mathcal{V}_{\text{halo}} = 2\pi r_{\text{MW}}^2 h$  with  $r_{\text{MW}} = 20 \text{ kpc}$  and  $h = 4 \text{ kpc}$ , we obtain the Galactic CR proton luminosity per logarithmic energy,

$$E \frac{dU_{\text{cr}}}{dE} \frac{\mathcal{V}_{\text{halo}}}{t_{\text{esc}}(E)} \sim 2 \times 10^{40} \text{ erg s}^{-1} \left( \frac{E}{10 \text{ GeV}} \right)^{-0.39}, \tag{7}$$

consistent with Eqs. (4) and (5). Equations (4) and (7) may not be fully independent because  $D$  and  $h$  are usually determined by exploiting a propagation model and using information on the ratio of secondary and primary CR fluxes. The advantage of Eq. (4), over Eq. (7), is that the CR luminosity is expressed with  $M_{\text{gas}}$  and  $X_{\text{esc}}$  that do not explicitly refer to the uncertain CR halo size,  $h$ . Here it is more useful to show both derivations to see its consistency with the traditional expression [i.e., Eq. (7)].

## 3. Global cosmic-ray energy generation rate density

With the CR dominantly produced in ccSNe we may assume that its energy generation rate density is proportional to the star-formation rate  $\psi$ . We may take the star-formation rate of the Milky Way,  $\psi_{\text{MW}} \approx 1.7 \pm 0.2 M_{\odot} \text{ yr}^{-1}$  [26], which is consistent with the global value at  $z = 0$ ,  $\psi = 0.015 M_{\odot} \text{ Mpc}^{-3} \text{ yr}^{-1}$  [39] within a factor of 2, when scaled the Milky Way luminosity to the global luminosity density of galaxies.

Using Eq. (4), the global CR energy generation rate density, or simply CR luminosity density,  $Q_{\text{cr}}$  is given per logarithmic energy, as

$$E \frac{dQ_{\text{cr}}}{dE} = \frac{dQ_{\text{cr}}}{d \ln E} = \frac{\psi}{\psi_{\text{MW}}} \frac{dL_{\text{cr}}}{d \ln E} \simeq 10^{45.9 \pm 0.3} \text{ erg Mpc}^{-3} \text{ yr}^{-1} \left( \frac{E}{10 \text{ GeV}} \right)^{2-s_{\text{cr}}}, \quad (8)$$

including the helium contribution.

The result is shown in Fig. 1 in the (grey) shaded region for  $E < 3 \text{ TeV}$ , where the AMS-02 data are available. A factor of 4 uncertainty is implied here to represent various uncertainties, such as the CR density enhancement around the Galactic center region, the gas mass estimate, star-formation rate, and so on. The calculation with the single power-law grammage with  $\delta = 0.4$  is shown with the double dashed lines, which differ little from the broken power-law case shown with the solid lines, showing impacts of a different power-law index. In this figure, we also depict the UHE CR from Auger, the gamma-ray luminosity density from the *Fermi* Large Area Telescope [8], and the high-energy neutrino luminosity density from IceCube [9], to compare them with the CR luminosity density, as we discuss in later subsections. Table I summarizes the luminosity and energy densities of high-energy cosmic particles.

Our results imply that the source spectral index for the proton component is larger than the nominal value expected by the diffusive shock acceleration mechanism for non-relativistic quasiparallel shocks (i.e.,  $s_{\text{cr}} = 2.0$ ). Our larger

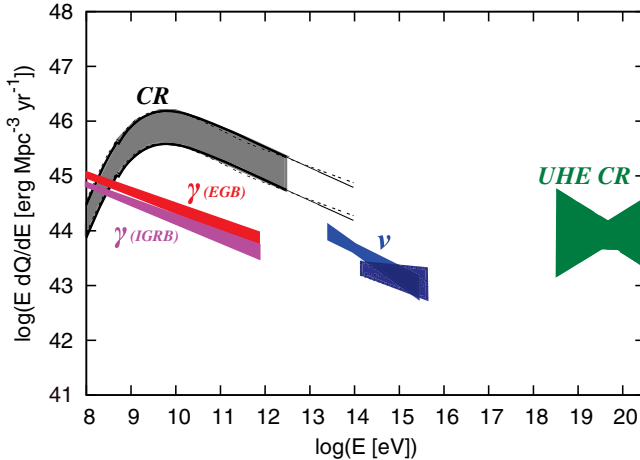


FIG. 1. Local ( $z = 0$ ) CR energy generation rate density estimated from the AMS-02, Voyager and other relevant CR data. UHE CR luminosity density is based on the Auger experiment. High-energy neutrino and gamma-ray luminosity densities use IceCube and *Fermi* Large Area Telescope, respectively. With the IceCube data both results from the global analysis and the upgoing muon neutrino analysis are included. For gamma rays, both total “extragalactic gamma-ray background” (EGB: including resolved gamma-ray sources) and “isotropic diffuse gamma-ray background (IGRB)” are displayed. The star-formation history is assumed for the neutrino and gamma-ray luminosity densities as discussed in the text.

TABLE I. Luminosity densities  $Q$  in units of  $\text{erg Mpc}^{-3} \text{ yr}^{-1}$  and energy densities  $\Omega$  in units of the critical density  $\rho_{\text{crit}} c^2$  of CRs, UHE CRs, high-energy neutrinos, and gamma rays, integrated over energies. For redshift evolution, the star-formation rate history is assumed, as discussed in the text.

|          | CR          | UHE CR       | $\nu$ (global) | $\nu$ (upgoing) | $\gamma$ (total) | $\gamma$ (IGRB) |
|----------|-------------|--------------|----------------|-----------------|------------------|-----------------|
| $Q$      | $10^{46.6}$ | $10^{44.5}$  | $10^{44.3}$    | $10^{43.8}$     | $10^{45.52}$     | $10^{45.31}$    |
| $\Omega$ | $10^{-8.3}$ | $10^{-11.5}$ | $10^{-10.7}$   | $10^{-11.2}$    | $10^{-9.44}$     | $10^{-9.64}$    |

index is consistent with the recent result based on the leaky box model [40], and the observations of young supernova remnants such as Cas A [41]. Such a steeper spectrum might point to additional processes that may play a role in the CR acceleration (e.g., [42–45]).

We remark that  $s_{\text{cr}} \approx 2.3\text{--}2.4$  derived from the AMS-02 experiment is the local spectral index. The CR spectral index may vary spatially across the Milky Way, which can be probed by gamma-ray observations. For instance, GeV gamma-ray observations suggest harder indices in the inner regions of the Milky Way [31]. Somewhat a harder global index such as  $s_{\text{cr}} \sim 2.2$  may be allowed by the anisotropic diffusion [46], although indices required for the perpendicular diffusion,  $\delta \sim 0.5$ , seem larger than the value suggested by the AMS-02 experiment [18]. On the other hand, a relatively soft spectrum with  $s_{\text{cr}} \sim 2.4$  is also inferred from the gamma-ray data of the starburst galaxy Arp 220 [47]. The global index is by no means definitive in the state-of-the-art experiments. For this study we take the local value inferred from the AMS-02 experiment literally. We note that a 0.1 difference in the index causes a 0.5 dex change in the luminosity density at  $10^{19} \text{ eV}$  when extrapolated from  $10^{14} \text{ eV}$ . This is somewhat beyond what we tolerate at UHE energies.

## B. Extragalactic cosmic rays

UHE CRs that cannot be confined in the Milky Way would represent extragalactic CRs. To estimate the luminosity density, we assume that UHE CRs are composed dominantly of protons. The dominance of protons or light nuclei is suggested in the energy range near the ankle [6,7], and we find that this assumption would not result in too significant an error in our order of magnitude estimate. The UHE CR flux measured by Auger is written [48]

$$E^2 \Phi_{\text{uhecr}} = 2.43 \times 10^{-8} \text{ GeV cm}^{-2} \text{ s}^{-1} \text{ sr}^{-1} \left( \frac{E}{E_{\text{ankle}}} \right)^{2-\gamma_{\text{cr}}} \times \begin{cases} 1 & (E < E_{\text{ankle}}) \\ \left[ \frac{1+(E_{\text{ankle}}/E_{\text{supp}})^{\Delta\gamma_{\text{cr}}}}{1+(E/E_{\text{supp}})^{\Delta\gamma_{\text{cr}}}} \right] & (E \geq E_{\text{ankle}}) \end{cases} \quad (9)$$

where  $\gamma_{\text{cr}} = 3.29$  below the ankle energy  $E_{\text{ankle}} = (4.82 \pm 0.8) \times 10^{18} \text{ eV}$ , and  $\gamma_{\text{cr}} = 2.60$  above it;  $E_{\text{supp}} = (4.21 \pm 0.78) \times 10^{19} \text{ eV}$  is the energy of suppression and  $\Delta\gamma_{\text{cr}} = 3.1$ .

Using the observed UHE CR flux and their characteristic energy-loss lengths,  $ct_{\text{loss}} \sim 100\text{--}1000$  Mpc at  $E \sim 10^{19}\text{--}10^{20}$  eV, the UHE CR luminosity density is roughly

$$E \frac{dQ_{\text{uhecr}}}{dE} \approx \frac{4\pi E^2 \Phi_{\text{uhecr}}}{ct_{\text{loss}}} \simeq 0.9 \times 10^{44} \text{ erg Mpc}^{-3} \text{ yr}^{-1} \left( \frac{ct_{\text{loss}}}{1 \text{ Gpc}} \right)^{-1}. \quad (10)$$

at around  $E = 10^{19}$  eV. Calculations of the propagation following Refs. [49,50], taking into account energy losses due to the photonuclear and Bethe-Heitler processes, give

$$E \frac{dQ_{\text{uhecr}}}{dE} \approx 10^{43.8 \pm 0.2} \text{ erg Mpc}^{-3} \text{ yr}^{-1} C(s_{\text{cr}}) \left( \frac{E}{10^{19.5} \text{ eV}} \right)^{2-s_{\text{cr}}}, \quad (11)$$

where  $C(s_{\text{cr}}) = \max[1, s_{\text{cr}} - 1]$  for  $1.5 \lesssim s_{\text{cr}} \lesssim 2.5$ , being consistent with Refs. [51,52] within 50%. The result on the UHE CR luminosity density depends on the fitting range, which reflects details of modeling of the Galactic to extragalactic transition. It is slightly affected by the redshift evolution of sources, but is not very important, for UHE CRs from high redshift sources are attenuated by energy losses. The interpretation of the shower maximum in air-shower experiments is under debate, and the UHE CR composition is unclear due to uncertainties in hadronic interaction models. The UHE CR spectrum can be fitted not only by protons but also by medium heavy or heavy nuclei, and the composition also affects precise values of the UHECR generation rate density. However, because energy loss lengths of different nuclei are comparable at  $E \sim 10^{19}$  eV (e.g., [53]), their differential UHE CR generation rate densities are similar in this energy range. For example, at  $E \sim 10^{19}$  eV, energy loss lengths of nuclei lighter than nitrogen or oxygen are slightly shorter than that of protons. Heavier nuclei have longer but still comparable loss lengths thanks to unavoidable energy losses by the cosmic expansion, which results in somewhat smaller values of the UHE CR generation rate density. We take a factor of 2 uncertainty in this study, which is conservative if we hold the proton composition scenario.

The differential UHE CR luminosity density, depicted in Fig. 1 above, is of the order of  $\sim 10^{44}$  erg Mpc $^{-3}$  yr $^{-1}$ . The spectral index at the sources is assumed to be  $1.5 \leq s_{\text{cr}} \leq 2.5$ . We remark that the differential UHE CR luminosity density at  $\sim 3 \times 10^{19}$  eV that concerns us is not too sensitive to the source spectral index  $s_{\text{cr}}$ , which is not easy to infer due to the degeneracy with other parameters such as the redshift evolution (e.g., [54,55]) and extragalactic magnetic fields (e.g., [56,57]). This is also consistent with the fact that the cosmogenic neutrino flux at  $\sim 1$  EeV does not depend on  $s_{\text{cr}}$  and the maximum CR energy at least in the proton composition case (see Figs. 6

and 7 of Ref. [58]). Given these, one may suspect that the galactic CRs at low energies, when the leakage from galaxies is fully taken into account, may extrapolate to the UHE range around  $3 \times 10^{19}$  eV reasonably well: in fact, the two regions can match if the spectral index is effectively  $s_{\text{cr}} \approx 2.1\text{--}2.2$ .

Lower-energy CR, however, if extrapolated to high energies with the power-law index with  $s_{\text{cr}} \approx 2.33\text{--}2.39$  as derived from AMS-02, undershoots the UHECR luminosity density by an order of magnitude [59]. Matching of the low-energy and the high-energy components of CRs, requires tilting of the power law, say by anisotropic diffusion, reacceleration outside the galactic disc, or else, additional sources with a harder spectrum are needed. CRs cannot achieve UHE energies in remnants of ordinary ccSNe, so we focus on the latter two possibilities.

For active galactic nuclei (AGN), for instance, to be a valid candidate for such an additional agent, the requirement is that the CR luminosity density above TeV-PeV energies from additional sources overwhelm that from normal star-forming galaxies. The luminosity density of CRs generated in AGN is unknown for sure, but we see circumstantial evidence that the total CR luminosity density of AGN can be on the same order of magnitude as that from normal galaxies, as we argue in Appendix A 2. Not only AGN but a number of rival candidates would raise the luminosity density required for UHE CRs, as also discussed in Appendixes A 1 and A 3.

The luminosity density and the energy density are summarized in Table I. Both quantities are calculated by integrating over energies from  $E = 10^{18.5}$  eV to  $E = 10^{20.5}$  eV. We need to fix the slope of the spectrum: for example,  $s_{\text{cr}} = 2.0$  gives  $Q_{\text{uhecr}} \simeq 3.5 \times 10^{44}$  erg Mpc $^{-3}$  yr $^{-1}$ . If we extrapolate this UHE CR spectrum to  $E = 1$  GeV, we have  $Q_{\text{uhecr}} \simeq 10^{45.3}$  erg Mpc $^{-3}$  yr $^{-1}$ . With Eq. (9), we obtain  $\Omega_{\text{uhecr}} \simeq 10^{-11.5}$ , which is about  $\sim 10^{-3}$  of the total CR energy density.

### C. High-energy neutrinos

An analysis based on a global fit of the neutrino data measured in the IceCube experiment yields the flux [60]

$$E_{\nu}^2 \Phi_{\nu} = (6.7 \pm 1.2) \times 10^{-8} \text{ GeV cm}^{-2} \text{ s}^{-1} \text{ sr}^{-1} \times \left( \frac{E_{\nu}}{0.1 \text{ PeV}} \right)^{-0.50 \pm 0.09}, \quad (12)$$

in the 25 TeV–2.8 PeV range. Here neutrinos (and anti-neutrinos) are added over three flavors. This is consistent with neutrino-induced showers, which gives the neutrino spectrum  $\Phi_{\nu} \propto E_{\nu}^{-s}$  with  $s = 2.48 \pm 0.08$  [9].

The high-energy neutrino flux is also measured with upgoing muons in the 119 TeV–4.8 PeV region. Eight years of the IceCube data give [9]

$$E_\nu^2 \Phi_{\nu_\mu} = 1.01_{-0.23}^{+0.26} \times 10^{-8} \text{ GeV cm}^{-2} \text{ s}^{-1} \text{ sr}^{-1} \times \left( \frac{E_\nu}{0.1 \text{ PeV}} \right)^{-0.19 \pm 0.10} \quad (13)$$

per neutrino flavor. A global fit of neutrino data gives a softer spectrum, and this is also true in the analyses of neutrino-induced showers and high-energy starting events [9].

The arrival direction of high-energy neutrinos is consistent with isotropic, which constrains the Galactic contribution, and points to predominantly extragalactic nature of sources for IceCube neutrinos [9,61].

The differential neutrino luminosity density is

$$E_\nu \frac{dQ_\nu}{dE_\nu} \approx \frac{4\pi E_\nu^2 \Phi_\nu}{c \xi_z t_H} \simeq 10^{43.3 \pm 0.1} \text{ erg Mpc}^{-3} \text{ yr}^{-1} \left( \frac{2}{\xi_z} \right) \times \left( \frac{E_\nu^2 \Phi_\nu}{3 \times 10^{-8} \text{ GeV cm}^{-2} \text{ s}^{-1} \text{ sr}^{-1}} \right), \quad (14)$$

where  $\xi_z = t_H^{-1} \int \frac{dz}{1+z} \left| \frac{dt}{dz} \right| (Q_\nu(z)/Q_\nu) \approx 2$  is the correction factor for the integration over redshift with the star-formation history we adopt [39]. We note that the line-of-sight integral in the diffuse flux calculation is dominated by sources at  $z \sim 1$ . The neutrino luminosity densities derived from the IceCube data are also presented in Fig. 1 above. Equation (13) is multiplied by a factor of 3 in the figure to take into account the other flavors.

The global analysis of the  $\gtrsim 10$ –30 TeV neutrino data gives  $Q_\nu \simeq 1.8 \times 10^{44} \text{ erg Mpc}^{-3} \text{ yr}^{-1} (2/\xi_z)$ , and the upgoing muon neutrino analysis focusing on  $\gtrsim 100$  TeV leads to  $Q_\nu \simeq 5.6 \times 10^{43} \text{ erg Mpc}^{-3} \text{ yr}^{-1} (2/\xi_z)$  (see Table I). The former is by a factor of 3 larger because of the higher neutrino flux in the 10–30 TeV range. If the neutrino spectrum is extended to lower energies with  $s \sim 2.5$ –3.0, both  $Q_\nu$  and  $\Omega_\nu$  will be even larger.

High-energy neutrinos are produced by CRs through inelastic  $pp$  or  $p\gamma$  interactions, yielding the energy flux (e.g., [62,63]),

$$E_\nu^2 \Phi_\nu^{(pp/p\gamma)} \approx \frac{c \xi_z t_H}{4\pi} \frac{3K}{4(1+K)} \min[1, f_{\text{meson}}] E_p \frac{dQ_{\text{excr}}}{dE_p}, \quad (15)$$

where  $K = 1$  or  $2$  for  $p\gamma$  or  $pp$  interactions, respectively, and  $f_{\text{meson}}$  is the effective optical depth for the meson production. With  $E_\nu^2 \Phi_\nu = E_\nu^2 \Phi_\nu^{(pp/p\gamma)}$  we are led to a constraint on the CR luminosity density at energies relevant to IceCube neutrinos:

$$E_p \frac{dQ_{\text{excr}}}{dE_p} \approx 4.4 \times 10^{43} \text{ erg Mpc}^{-3} \text{ yr}^{-1} \frac{[4(1+K)/6K]}{\min[1, f_{\text{meson}}]} \times \left( \frac{2}{\xi_z} \right) \left( \frac{E_\nu^2 \Phi_\nu}{3 \times 10^{-8} \text{ GeV cm}^{-2} \text{ s}^{-1} \text{ sr}^{-1}} \right). \quad (16)$$

Imposing  $\min[1, f_{\text{meson}}] \leq 1$  gives a lower limit on the differential CR luminosity density [3]. At a few PeV energies, this is on the correct order of magnitude of the CR luminosity densities extrapolated from either the GeV–TeV range or UHE range.

#### D. High-energy gamma rays

The *Fermi* Large Area Telescope has identified a large number of extragalactic gamma-ray sources that consist of blazars, radio galaxies, and actively star-forming galaxies, but also it gives the “extragalactic gamma-ray background (EGB)” above 0.1 GeV [8], as

$$E_\gamma^2 \Phi_\gamma = (1.48 \pm 0.09) \times 10^{-6} \text{ GeV cm}^{-2} \text{ s}^{-1} \text{ sr}^{-1} \times \left( \frac{E_\gamma}{0.1 \text{ GeV}} \right)^{-0.31 \pm 0.02}. \quad (17)$$

At  $\gtrsim 50$  GeV energies one considers that the EGB is dominated by unresolved point sources, mainly of blazars [64–66]. The remaining background, including both unresolved point sources and diffuse component, is referred as the “isotropic diffuse gamma-ray background (IGRB)”. The IGRB flux up to  $\sim 1$  TeV is [8]

$$E_\gamma^2 \Phi_\gamma = (0.95 \pm 0.08) \times 10^{-6} \text{ GeV cm}^{-2} \text{ s}^{-1} \text{ sr}^{-1} \times \left( \frac{E_\gamma}{0.1 \text{ GeV}} \right)^{-0.32 \pm 0.02}. \quad (18)$$

As in Eq. (14), the gamma-ray background flux can be translated into the differential gamma-ray luminosity density

$$E_\gamma \frac{dQ_\gamma}{dE_\gamma} \approx \frac{4\pi E_\gamma^2 \Phi_\gamma}{c \xi_z t_H} \simeq 10^{43.86 \pm 0.05} \text{ erg Mpc}^{-3} \text{ yr}^{-1} \left( \frac{2}{\xi_z} \right) \times \left( \frac{E_\gamma^2 \Phi_\gamma}{10^{-7} \text{ GeV cm}^{-2} \text{ s}^{-1} \text{ sr}^{-1}} \right), \quad (19)$$

which gives  $Q_\gamma \simeq 3.3 \times 10^{45} \text{ erg Mpc}^{-3} \text{ yr}^{-1} (2/\xi_z)$  for the total EGB and  $Q_\gamma \simeq 2.1 \times 10^{45} \text{ erg Mpc}^{-3} \text{ yr}^{-1} (2/\xi_z)$  for the IGRB. The gamma-ray luminosity densities derived from the EGB and IGRB are also shown in Fig. 1.

Gamma rays are produced by leptonic processes such as the inverse-Compton radiation in addition to hadronic processes of  $pp$  and  $p\gamma$  interactions. For the hadronic

component the generated energy flux of gamma rays from neutral pion decay is, similarly to Eq. (15),

$$E_\gamma^2 \Phi_\gamma^{(pp/p\bar{p})} \approx \frac{c \xi_z t_H}{4\pi} \frac{1}{1+K} \min[1, f_{\text{meson}}] E_p \frac{dQ_{\text{excr}}}{dE_p}. \quad (20)$$

The fact that the EGB and IGRB receive both leptonic and hadronic contributions means  $E_\gamma^2 \Phi_\gamma^{(pp/p\bar{p})} \leq E_\gamma^2 \Phi_\gamma$ , which leads to an upper limit

$$E_p \frac{dQ_{\text{excr}}}{dE_p} \lesssim 2.2 \times 10^{44} \text{ erg Mpc}^{-3} \text{ yr}^{-1} \frac{[(1+K)/3]}{\min[1, f_{\text{meson}}]} \times \left(\frac{2}{\xi_z}\right) \left(\frac{E_\gamma^2 \Phi_\gamma}{10^{-7} \text{ GeV cm}^{-2} \text{ s}^{-1} \text{ sr}^{-1}}\right). \quad (21)$$

Equation (21) is valid for gamma rays in the GeV range. Very high-energy gamma rays with  $E_\gamma \gtrsim 0.1$  TeV, however, interact with the extragalactic background light (EBL) and cosmic microwave background (CMB), causing electron-positron pair creation. The generated electrons and positrons lose their energies through inverse-Compton scattering, producing electromagnetic cascades, whose resulting gamma rays appear in the MeV–TeV region. The spectrum of gamma rays may be characterized effectively with  $G_\gamma$ , the ratio of the differential energy spectrum of cascade gamma rays at specific energy  $E_\gamma$  to the integrated energy spectrum of injected gamma rays, electrons and positrons [67,68], such that  $E_\gamma (dG_\gamma/dE_\gamma) \equiv E_\gamma^2 \phi_\gamma^{(\text{cas})} / \int dE_\gamma E_\gamma \phi_\gamma^{(\text{em})}$ ,

$$\frac{dG_\gamma}{dE_\gamma} \propto \begin{cases} (E_\gamma/E_\gamma^{\text{br}})^{-1/2} & (E_\gamma \leq E_\gamma^{\text{br}}) \\ (E_\gamma/E_\gamma^{\text{br}})^{1-\beta} & (E_\gamma^{\text{br}} < E_\gamma \leq E_\gamma^{\text{cut}}). \end{cases} \quad (22)$$

where  $dG_\gamma/dE_\gamma$  is normalized as  $\int dE_\gamma (dG_\gamma/dE_\gamma) = 1$ ; the break energy  $E_\gamma^{\text{br}} \approx (4/3)(E_\gamma^{\text{cut}}/m_e c^2)^2 \epsilon_{\text{CMB}} \approx 0.034 \text{ GeV} (E_\gamma^{\text{cut}}/0.1 \text{ TeV})^2 [(1+z)/2]^2$  with  $\epsilon_{\text{CMB}}$  the CMB energy,  $E_\gamma^{\text{cut}}$  is the cutoff due to EBL and the spectral index  $\beta \sim 2$ . Averaging over redshifts,  $E_\gamma^{\text{br}} (d\bar{G}_\gamma/dE_\gamma)|_{E_\gamma^{\text{br}}} \sim (2 + \ln(E_\gamma^{\text{cut}}/E_\gamma^{\text{br}}))^{-1} \sim 0.1$ , which is consistent with a numerical calculation [68]. The detail of initial spectra is unimportant for they are largely washed out.

Electromagnetic cascades convert the bolometric electromagnetic energy, when input at sufficiently high energies, to lower-energy gamma rays in the *Fermi* range. The resulting gamma-ray background flux is [68]

$$E_\gamma^2 \Phi_\gamma^{(\text{cas})} \approx \frac{c \xi_z t_H}{4\pi} Q_\gamma^{(\text{em})} E_\gamma \frac{d\bar{G}_\gamma}{dE_\gamma}, \quad (23)$$

where  $Q_\gamma^{(\text{em})} \approx 4\pi \int dE_\gamma \Phi_\gamma^{(\text{em})} / (c \xi_z t_H)$  is the electromagnetic luminosity density due to the photomeson production

and the Bethe-Heitler pair production. Using Eqs. (18) and (23), one obtains [52,68]

$$Q_\gamma^{(\text{em})} \lesssim 8 \times 10^{44} \text{ erg Mpc}^{-3} \text{ yr}^{-1} (2/\xi_z) \times \left(\frac{E_\gamma^2 \Phi_\gamma}{10^{-7} \text{ GeV cm}^{-2} \text{ s}^{-1} \text{ sr}^{-1}}\right), \quad (24)$$

which is taken as an upper limit on the UHE CR luminosity density, since the effective optical depth is  $\gtrsim 1$  for the photomeson and the Bethe-Heitler pair production of UHE CRs above  $E \gtrsim 10^{18.5} \text{ eV}$ .

### III. ENERGY DENSITY OF COSMIC RADIATIONS

With the generation rate density  $Q_{\text{cr}}$ , the CR energy density is

$$E \frac{dU_{\text{cr}}}{dE} = E \frac{d\Omega_{\text{cr}}}{dE} (q_{\text{crit}} c^2) \approx \int^{t_{\text{surv}}} \frac{dt}{1+z} E' \frac{dQ_{\text{cr}}}{dE}, \quad (25)$$

where  $E' = (1+z)E$  and  $t_{\text{surv}} \approx \min[t_H, t_{\text{loss}}]$  is the survival time. In the absence of energy losses during the Hubble time,

$$E \frac{d\Omega_{\text{cr}}}{dE} \approx \frac{\xi_z t_H}{q_{\text{crit}} c^2} E \frac{dQ_{\text{cr}}}{dE} \simeq 10^{-9.1 \pm 0.3} \left(\frac{E}{10 \text{ GeV}}\right)^{2-s_{\text{cr}}} (\xi_z/2), \quad (26)$$

where  $\xi_z = t_H^{-1} \int \frac{dz}{1+z} \left| \frac{dt}{dz} \right| (Q_{\text{cr}}(z)/Q_{\text{cr}}) \approx 2$  is introduced as in Sec. II. Integrating over energies, we obtain the global CR energy density in units of the critical energy density,  $q_{\text{crit}} c^2$ ,

$$\Omega_{\text{cr}} = U_{\text{cr}} / (q_{\text{crit}} c^2) \simeq 10^{-8.3 \pm 0.3} (\xi_z/2), \quad (27)$$

in agreement with Ref. [1].

Figure 2 shows the cosmic energy density of CRs per logarithmic energy,  $d\Omega_{\text{cr}}/d \ln E$ , translated from Fig. 1. The upper (grey) shaded region is the global CR energy density, corresponding to the upper curves in Fig. 1. We also show the energy density of CRs that reside in the galactic disc, discarding the escaped CRs, with (brown) shades in the lower part of the figure. If, as in our archetype argument, the CRs generated in a galaxy escape, then the energy density of confined CRs amounts to  $t_{\text{esc}}(E) / (\xi_z t_H)$  times the above estimate. Here it is assumed that Eq. (6), given for the Milky Way, represents the typical escape time of galactic CRs.

In reality, low-energy CRs may undergo adiabatic energy losses in the expanding wind [69] and inelastic  $pp$  collisions, in particular, in actively star-forming galaxies (starburst galaxies), in which the  $pp$  cooling time is likely

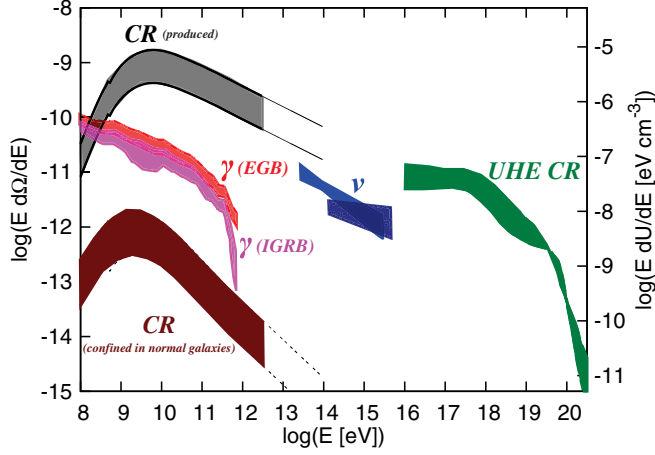


FIG. 2. Local ( $z = 0$ ) energy densities of cosmic particles (in unit of  $\rho_{\text{crit}} c^2$  for the left axis). We ignore possible energy losses of CRs injected in the past. Unavoidable energy losses of UHE CRs are taken into account, and we show both proton ankle and mixed composition models. The energy density of CRs confined in normal galaxies is indicated assuming  $t_{\text{esc}} = 15\text{--}100$  Myr at  $R = 1$  GV. The softening of the EGB and IGRB spectra is caused by the attenuation by the extragalactic background light.

to be shorter than the advection and the escape times [70,71]. Thus, whereas the above estimate, corresponding to the upper curve in Fig. 2, may be valid in normal galaxies, this  $\Omega_{\text{cr}}$  we obtained is taken, for sure, as an upper limit on the current energy density of CRs with stellar origins.

For extragalactic radiations, including UHE CRs, neutrinos, and gamma rays, the differential global energy density is written in terms of the observed energy density as,

$$E \frac{d\Omega}{dE} = E \frac{dU}{dE} \frac{1}{\rho_{\text{crit}} c^2} = \frac{4\pi E^2 \Phi}{c} \frac{1}{\rho_{\text{crit}} c^2}. \quad (28)$$

The UHE CR energy density on Earth is measured accurately, but the global energy density depends on the transition from Galactic to extragalactic CRs. In Fig. 2, the upper curve of the UHE CR shade region is taken from Ref. [57] which uses the mixed composition model with the proton dominance around the ankle energy. For  $E \gtrsim 10^{18.5}$  eV this model has the spectrum that is close to the flux given by Eq. (9). The lower curve of the (green) shade region is based on the classical proton ankle model with  $s_{\text{sc}} = 2.0$  [52,72], which can be taken as a more conservative estimate on the UHE CR energy density. Note that both curves agree with each other above  $E \sim 10^{19}$  eV, where the extragalactic component is dominant.

High-energy neutrino observations serve as a probe for the differential luminosity and energy density of CRs. For a given spectral index we obtain the total luminosity density: for  $s = 2.5$  we have  $Q_{\nu} \simeq 10^{44.3 \pm 0.1}$  erg Mpc $^{-3}$  yr $^{-1}$  ( $2/\xi_z$ ) and  $\Omega_{\nu} \gtrsim 10^{-10.7 \pm 0.1}$  above 25 TeV (see Table I).

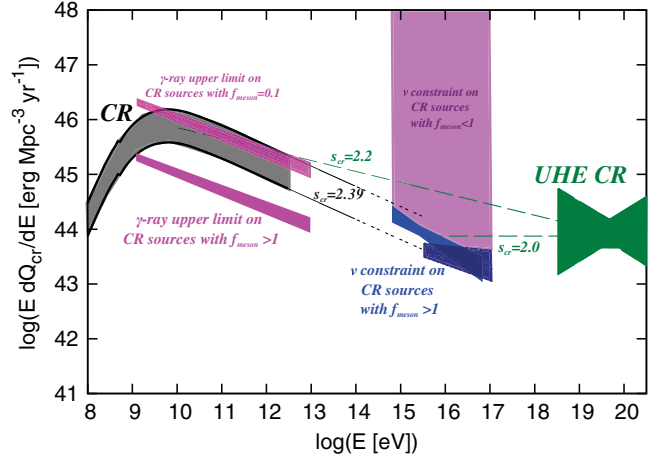


FIG. 3. Similar to Fig. 1, but neutrino and gamma-ray luminosity densities are converted into CR energy generation rate densities assuming that they are produced by inelastic  $pp$  interactions. The high-energy neutrino background gives constraints on the CR energy generation rate density, while the IGRB is taken as an upper limit for a given value of the effective optical depth to meson production ( $f_{\text{meson}}$ ): the cases for  $f_{\text{meson}} \geq 1$  and  $f_{\text{meson}} = 0.1$  are displayed.

This yields  $Q_{\text{excr}} \gtrsim 10^{44.6 \pm 0.1}$  erg Mpc $^{-3}$  yr $^{-1}$  ( $2/\xi_z$ ) and  $\Omega_{\text{excr}} \gtrsim 10^{-10.4 \pm 0.1}$  above  $E_p \sim 0.5$  PeV, assuming inelastic  $pp$  interactions being the dominant process.

As indicated in Fig. 3 below, the GeV–TeV CR spectrum extrapolated to PeV energies can be compatible with the soft CR spectrum indicated by the 10–100 TeV neutrino data if the meson production is fully efficient for PeV CRs, i.e., the effective optical depth  $f_{\text{meson}} \gtrsim 1$ . On the other hand,  $\Omega_{\text{cr}} \gg \Omega_{\gamma}$  means that the CR energy density in the GeV–TeV range needed to explain GeV–TeV gamma rays overshoots the observed CR roughly by a factor of 3–10 (see Fig. 3). This implies that the gamma-ray production for GeV–TeV CRs should not be fully efficient (i.e.,  $f_{\text{meson}} \ll 1$ ) and/or the hadronic gamma rays are attenuated by interactions with ambient matter or radiation. A comparison of the IceCube and *Fermi* data implies that the CR accelerators are hidden when viewed in GeV–TeV gamma rays [62].

## IV. DISCUSSION

### A. Cosmic-ray reacceleration in star-forming galaxies

The CR energy generation rate density in the GeV–TeV range, when leaked CRs are included, is not much different from that in the UHE range, across energies 10 orders of magnitude apart. This may point towards the idea that CRs may be reaccelerated by the Fermi acceleration in the vicinity of galaxies, say, in superbubbles or galactic winds driven by the star formation, whose power-law index can be  $s_{\text{cr}} \sim 2$  or smaller [73,74].

The velocity of galactic winds driven by the star formation can be  $V_s \sim 300\text{--}1000$  km s $^{-1}$  [75,76] (see also



reviews, e.g., [77,78]), and the termination shock radius would be  $R_s \sim 5\text{--}50$  kpc (e.g., [69]). The Fermi bubbles, which are seen in gamma rays, could be attributed to the termination shock formed by starburst winds. With a magnetic field of  $B \sim 5 \mu\text{G}$  [69,79], the maximum energy of CRs is

$$E_{\max} \approx \frac{3}{20} ZeB(V_s/c)R_s \sim 10^{16} \text{ eV} Z \left( \frac{B}{5 \mu\text{G}} \right) \left( \frac{V_s}{1000 \text{ km s}^{-1}} \right) \left( \frac{R_s}{5 \text{ kpc}} \right), \quad (29)$$

which means that galactic CRs in the halo can be reaccelerated up to or even beyond the knee energy  $\approx 3\text{--}4$  PeV. The Galactic CR spectrum may be explained by the reacceleration of cosmic rays originating from supernovae.

The actively star-forming galaxies, often referred to as starburst galaxies, may have a higher wind velocity of  $V_s \sim 1000\text{--}2000 \text{ km s}^{-1}$  [75,80] and a larger magnetic field of  $B \sim 0.1\text{--}1 \text{ mG}$  [81], with which the maximum energy could reach  $E_{\max} \sim 10^{20.5} (Z/26) \text{ eV}$ . This value is significantly higher than that for the Milky Way. Thus, if galactic CRs can be reaccelerated in the galactic halo with a hard spectral index of  $s_{\text{cr}} \sim 2.0\text{--}2.2$ , it is possible that the global CR generation rate density in the GeV–TeV range could match that in the UHE range, up to one order of magnitude across the energy difference extending 10 orders of magnitude. In this scenario, the highest-energy CRs are largely nuclei and the correlation between UHE CRs and starburst galaxies can be expected.

### B. Active galactic nuclei and structure formation shocks

As detailed in Appendix A 2, recent observations revealed that luminosity densities of nonthermal gamma-ray emissions from AGN, including blazars, lie in the range  $Q_{\gamma}^{\text{AGN}} \sim 3 \times (10^{44} - 10^{46}) \text{ erg Mpc}^{-3} \text{ yr}^{-1}$ . The observed x-ray and gamma-ray emissions are attributed to synchrotron and inverse-Compton radiation from relativistic electrons. We expect that ions may also be accelerated by the Fermi acceleration mechanism, so that the CR luminosity density for AGN may be comparable to or even larger than that for star-forming galaxies,  $Q_{\text{cr}} \approx 2 \times 10^{46} \text{ erg Mpc}^{-3} \text{ yr}^{-1}$ , as well as  $Q_{\gamma}^{\text{AGN}}$ . The gamma-ray luminosity densities for blazars and radio galaxies are similar to that for starburst galaxies,  $Q_{\gamma}^{\text{SBG}} \sim 3 \times 10^{44} \text{ erg Mpc}^{-3} \text{ yr}^{-1}$ , which is consistent with the idea that EGB consists of multiple components.

CRs may be accelerated by shocks in hierarchical structure formation, which induces accretion shocks, cluster and galaxy mergers. The integrated CR luminosity densities associated with these shocks are

$Q_{\text{cr}} \sim 3 \times (10^{45} - 10^{46}) \text{ erg Mpc}^{-3} \text{ yr}^{-1}$  (see Appendix A 3). This is also comparable to that for star-forming galaxies.

### C. Consistency among high-energy cosmic radiations?

In summary, Fig. 3 reiterates the energy generation rate density of CRs. In this figure, energies of high-energy neutrinos and gamma rays are those of primary CRs. IceCube neutrinos give constraints on the CR luminosity density in the 1–100 PeV range. In particular, for  $s_{\text{cr}} \sim 2.0\text{--}2.3$ , CR spectra extrapolated from UHE energies can match the CR luminosity needed to explain the IceCube data, if the efficiency to produce neutrinos is sufficiently high (i.e.,  $\min[1, f_{\text{meson}}] \sim 0.03\text{--}1$ ); see Fig. 3 and Eq. (16). The IGRB gives an upper limit on the CR luminosity density for a given  $f_{\text{meson}}$  [see Eq. (21)]; Fig. 3 displays the case for  $f_{\text{meson}} \geq 1$ . This upper limit becomes weaker if  $f_{\text{meson}} < 1$ . The figure indicates that hard CR spectra with  $s_{\text{cr}} \sim 2.0\text{--}2.2$  can explain the UHE CR and neutrino fluxes without violating the upper limits from the IGRB; see also Ref. [2].

That UHE CR flux around the ankle energy is compatible with those of 0.1 PeV neutrinos and 0.1 TeV gamma rays (see Fig. 2 above). This implies that the UHE CR luminosity density is comparable to the CR energy generation rate density to explain the high-energy neutrino background in the sub-PeV range and the IGRB in the sub-TeV range (see Fig. 3). This fact naturally leads to an idea that UHE CRs, neutrinos, and gamma rays may share a common origin. As an example, let us consider the CR luminosity density given by Eq. (11), which yields  $E(dQ_{\text{uhec}}/dE) \approx 0.75 \times 10^{44} \text{ erg Mpc}^{-3} \text{ yr}^{-1}$  for  $s_{\text{sr}} \sim 2$ . From Eq. (16), the IceCube neutrino flux can be explained if the following condition is met:

$$\min[1, f_{\text{meson}}] \sim 0.6[4(1+K)/6K](2/\xi_z). \quad (30)$$

With  $K = 2$  and  $\xi_z = 2$ , this means  $f_{\text{mes}} \sim 0.6$  (cf. Fig. 1 of Ref. [72]). Such high-energy neutrino sources also satisfy Eq. (21), since

$$\min[1, f_{\text{meson}}] \lesssim 3[(1+K)/3](2/\xi_z). \quad (31)$$

This implies that the gamma-ray flux from  $pp$  interactions is  $E_{\gamma}^2 \Phi_{\gamma} \sim 2 \times 10^{-8} \text{ GeV cm}^{-2} \text{ s}^{-1} \text{ sr}^{-1}$  with  $f_{\text{meson}} \sim 0.6$ . Including the cascade component that would enhance the flux by a factor of 2, we have  $E_{\gamma}^2 \Phi_{\gamma} \sim 4 \times 10^{-8} \text{ GeV cm}^{-2} \text{ s}^{-1} \text{ sr}^{-1}$ , as consistent with a numerical calculation [2]. UHE CRs also produce cosmogenic gamma rays during their propagation in intergalactic space. At  $E \gtrsim 10^{18.5} \text{ eV}$ ,  $\sim 65\% - 100\%$  of the UHE CR proton is converted to the electromagnetic energy. Thus, one finds that the IGRB constraint on  $Q_{\gamma}^{(\text{em})}$  [see Eq. (24)] is readily met, and the corresponding cosmogenic gamma-ray

flux is  $E_\gamma^2 \Phi_\gamma \sim 4 \times 10^{-8} \text{ GeV cm}^{-2} \text{ s}^{-1} \text{ sr}^{-1}$ . Summing up contributions originating from  $pp$  interactions in the source and  $p\gamma$  interactions in intergalactic space, the total gamma-ray flux is  $E_\gamma^2 \Phi_\gamma \sim 8 \times 10^{-8} \text{ GeV cm}^{-2} \text{ s}^{-1} \text{ sr}^{-1}$  (at  $\sim 10 \text{ GeV}$ ), which matches the nonblazar component of the EGB [8,66]. (We note that the sub-TeV spectrum of the EGB is affected by gamma-ray attenuation due to the extragalactic background light.) This result also agrees with Fig. 1 of Ref. [72], and the CR spectral index needs to be  $s_{\text{cr}} \lesssim 2.1$  in simple power-law models (see also Ref. [57], in which such a hard CR index is effectively achieved for CRs leaving their accelerators). A hard CR spectrum extrapolated from UHE energies downwards can simultaneously account for high-energy neutrinos and gamma rays. UHE CRs may come from either reacceleration of galactic CRs in the halo or additional source population.

## V. SUMMARY

We have studied energy generation rate densities and energy densities of nonthermal cosmic particles, using the recent experiments of CRs at both GeV–TeV region and ultrahigh energies, and in addition high-energy neutrinos and gamma rays. The total energy density of GeV–TeV CRs is  $\Omega_{\text{cr}} \simeq 10^{-8.3}$ . Extrapolation to UHE energies, across the energy range of 10 orders of magnitude, gives, if we would adopt the local CR spectral index derived from the AMS-02 experiment at GeV–TeV energies, nominally a value smaller than the observed UHE CR luminosity density by a factor of  $\sim 30$ . That is, the UHE CRs do not quite match the extrapolation from the GeV–TeV CRs if the global CR spectral index is the same as the local one,  $s_{\text{cr}} \approx 2.3\text{--}2.4$ . The matching requires somewhat harder spectra, say  $s_{\text{cr}} \approx 2.1\text{--}2.2$ .

The gap between GeV–TeV CRs and UHE CRs leaves room for reacceleration of GeV–TeV CRs, or additional components contributing to the high-energy CRs. In fact, the energy stored in circumgalactic and cluster warm matter is  $\Omega \simeq 10^{-8.0 \pm 0.2}$  [1]. This is larger than the total energy density of CRs, so that it can be used to reaccelerate CRs. Alternatively, we can think of a number of candidate sources that would fill the gap, such as AGN and/or similar active objects, or some violent transients that have comparable energies when integrated over time. We argue that it is energetically possible that any of such sources could fill the gap. For the moment, we are unable to distinguish between the two possibilities, or single out some candidate sources.

It is interesting to observe that high-energy cosmic neutrinos and gamma rays indicate the relevant luminosity densities that are, roughly speaking, comparable to that of the UHE CRs. In fact, the observed high-energy neutrino flux is consistent with extragalactic CRs, but the CRs needed to produce gamma rays, at an estimate of the maximum meson production efficiency, should be smaller than GeV–TeV CRs. The gamma-ray production may be

suppressed effectively, say, by small effective optical depths for meson production and/or by large optical depths to two photon annihilation. As a global picture, our energetics argument is suggestive of a common origin of UHE CRs, high-energy neutrinos and gamma rays [57].

## ACKNOWLEDGMENTS

We thank Kfir Blum and Yutaka Ohira for discussions on cosmic-ray propagation and interpretations of the spectral hardening. We also thank Eli Waxman for discussion as to the origin of IceCube neutrinos below 100 TeV. The work of K. M. is supported by the Alfred P. Sloan Foundation and the U.S. National Science Foundation (NSF) under National Science Foundation Grant No. PHY-1620777. He also thanks the Institute for Advanced Study for its hospitality during the work. M. F. thanks Hans Böhringer and the late Yasuo Tanaka for the hospitality at the Max-Planck-Institut für Extraterrestrische Physik and also Eiichiro Komatsu at Max-Planck-Institut für Astrophysik, in Garching. He also wishes to thank Alexander von Humboldt Stiftung for the support during his stay in Garching and the Monell Foundation in Princeton. He received in Tokyo Grant-in-Aid (No. 15430000110) from the Ministry of Education. Kavli I. P. M. U. is supported by a World Premier International Research Centre Initiative of the Ministry of Education, Japan.

## APPENDIX: LUMINOSITY DENSITY OF VARIOUS SOURCES

We discuss here a number of candidate sources that may contribute significantly to CRs, with the fact in mind that robust estimates for their CR energy generation rate density are difficult with the present knowledge and, hence, they remain as order of magnitude estimates (see Table II for a summary of luminosity densities of photons or CRs).

We write the luminosity density  $Q(z)$  at  $z$  of some astrophysical source,

$$Q(z) = \int dL L \frac{dn_s}{dL}(L, z), \quad (\text{A1})$$

where  $n_s = \int dL (dn_s/dL)$  is the number density of the source per comoving volume. For the transient source, we write the luminosity density,

$$Q(z) = \int d\mathcal{E} \mathcal{E} \frac{d\rho_s}{d\mathcal{E}}(\mathcal{E}, z), \quad (\text{A2})$$

where  $\mathcal{E}$  is the energy and  $\rho_s = \int d\mathcal{E} (d\rho_s/d\mathcal{E})$  is the number of the transient sources per comoving volume per time (rate density). We denote their local luminosity density as  $Q$ .

### 1. Energetic transients in star-forming galaxies

Our result in the main text (Table I above) shows the luminosity density of galactic CRs,

TABLE II. The luminosity density  $Q$  in units of  $\text{erg Mpc}^{-3} \text{yr}^{-1}$  and the rate density  $\rho$  in units of  $\text{Mpc}^{-3} \text{yr}^{-1}$  or number density  $n$  in units of  $\text{Mpc}^{-3}$ , as discussed in the text: core-collapse supernova (ccSNe), hypernovae (HN), double neutron star mergers (DNS), gamma-ray bursts (GRB), low-luminosity gamma-ray bursts (LL GRB), tidal disruption events (TDE), BL Lac objects (BL Lac), flat-spectrum radio quasars (FSRQ), radio galaxies (RG), and accretion or merger shocks due to the cosmic structure formation (Accr/Mger). CR luminosity densities are those estimated from kinetic luminosity densities assuming  $\epsilon_{\text{cr}} = 0.1$ . For GRB and TDE the  $\gamma$ -ray luminosity densities are based on the BATSE and the *Swift* band observations. For BL Lac and FSRQ data are taken from *Fermi* Large Area Telescope observations.

|  | ccSN (CR)        | HN (CR)             | DNS (CR)              | GRB ( $\gamma$ )    | LL GRB ( $\gamma$ ) | TDE ( $\gamma$ )    |
|--|------------------|---------------------|-----------------------|---------------------|---------------------|---------------------|
| $Q$ [ $\text{erg Mpc}^{-3} \text{yr}^{-1}$ ] | $10^{46.6}$      | $10^{45.5}$         | $10^{44.5}$           | $10^{43.6}$         | $10^{43.5}$         | $10^{43.5}$         |
| $\rho$ [ $\text{Mpc}^{-3} \text{yr}^{-1}$ ]  | $10^{-4}$        | $10^{-5.5}$         | $10^{-5.8}$           | $10^{-9}$           | $10^{-6.5}$         | $10^{-10.5}$        |
|  | SBG ( $\gamma$ ) | AGN (X)             | BL Lac ( $\gamma$ )   | FSRQ ( $\gamma$ )   | RG ( $\gamma$ )     | Accr/Mger (CR)      |
| $Q$ [ $\text{erg Mpc}^{-3} \text{yr}^{-1}$ ] | $10^{44.5}$      | $10^{46.3}$         | $10^{45.4}$           | $10^{44.3}$         | $10^{44.6}$         | $10^{46.5}$         |
| $n$ [ $\text{Mpc}^{-3}$ ]                    | $10^{-4}$        | $10^{-4} - 10^{-3}$ | $10^{-7} - 10^{-6.5}$ | $10^{-9} - 10^{-8}$ | $10^{-5} - 10^{-4}$ | $10^{-6} - 10^{-5}$ |

$$Q_{\text{cr}} \sim 4 \times 10^{46} \text{ erg Mpc}^{-3} \text{yr}^{-1}. \quad (\text{A3})$$

This is compared with CRs to be generated in ccSNe showing that the two values are consistent; the bulk of CR can be ascribed to ccSNe.

In addition to ordinary ccSNe, rare but more energetic transients may occur, in particular, in star-forming galaxies, such as broadline Type Ibc supernovae, often called hypernovae with  $\mathcal{E}_{\text{HN}} \sim 10^{52}$  erg. The broadline Type Ibc rate is approximately  $\rho_{\text{HN}} \sim 3000 \text{ Gpc}^{-3} \text{yr}^{-1}$  [82], which is  $0.032 \pm 0.007$  times the ccSN rate. The CR luminosity density of hypernovae is then

$$Q_{\text{cr}}^{\text{HN}} \sim 3 \times 10^{45} \text{ erg Mpc}^{-3} \text{yr}^{-1} \epsilon_{\text{cr},-1} \mathcal{E}_{\text{HN},52}. \quad (\text{A4})$$

If  $s_{\text{cr}} \sim 2$  and the maximum energy  $E_{\text{max}} = 10^{20.5}$  eV, the differential UHE CR luminosity density  $E(dQ_{\text{cr}}^{\text{HN}}/dE) \sim 1 \times 10^{44} \text{ erg Mpc}^{-3} \text{yr}^{-1}$  is comparable to  $E(dQ_{\text{uhec}}/dE) \approx 0.75 \times 10^{44} \text{ erg Mpc}^{-3} \text{yr}^{-1}$  which is the UHE CR luminosity density given by Eq. (11).

One may suspect that Type Ia supernovae may also contribute to the CR generation. The rate of occurrence, however, is 1/20 that of ccSN, if integrated over the look back time to a higher redshift, and so their contribution to extragalactic CRs would be insignificant.

We have other events that may contribute to CRs. The recent detection of a double neutron star merger (DNS) suggests a rate density of  $\rho_{\text{DNS}} \sim 1540 \text{ Gpc}^{-3} \text{yr}^{-1}$  [83] with a large error. The kinetic energy of the ejecta is  $\mathcal{E}_{\text{ej}} \sim 2 \times 10^{51}$  erg. Their CR luminosity density, with the 10% CR efficiency assumption, is

$$Q_{\text{cr}}^{\text{DNS}} \sim 3 \times 10^{44} \text{ erg Mpc}^{-3} \text{yr}^{-1} \epsilon_{\text{cr},-1} \mathcal{E}_{\text{DNS},51.3}, \quad (\text{A5})$$

which could give an order of magnitude of UHE CRs.

Gamma-ray bursts (GRB) are also suggested as sources of UHE CRs [84,85]. The local rate density is estimated to be around  $\rho_{\text{GRB}} \sim 1 \text{ Gpc}^{-3} \text{yr}^{-1}$  [86,87]. With the *Swift* sample, the isotropic-equivalent gamma-ray energy is

$\mathcal{E}_{\text{isoy}} = 10^{52.3 \pm 0.7}$  erg [88], or  $\mathcal{E}_{\text{isoy}} \sim 10^{52.65}$  erg in the BATSE band. Then the gamma-ray luminosity of GRBs is

$$Q_{\text{MeV}\gamma}^{\text{GRB}} \sim 4 \times 10^{43} \text{ erg Mpc}^{-3} \text{yr}^{-1} \mathcal{E}_{\text{isoy},52.65}, \quad (\text{A6})$$

which is again comparable to the luminosity density of UHE CRs above the ankle.

It is considered that low-luminosity GRBs (LL GRB) form another population of gamma-ray transients. The rate density of low-luminosity GRBs, if associated with trans-relativistic supernovae with relativistic ejecta [89,90], is  $\rho_{\text{LLGRB}} \sim 100\text{--}1000 \text{ Gpc}^{-3} \text{yr}^{-1}$  [91,92]. With an isotropic-equivalent radiation energy  $\mathcal{E}_{\text{isoy}} \sim 10^{50}$  erg, the gamma-ray luminosity of low-luminosity GRBs is

$$Q_{\text{keV--MeV}\gamma}^{\text{LLGRB}} \sim 3 \times 10^{43} \text{ erg Mpc}^{-3} \text{yr}^{-1} \mathcal{E}_{\text{isoy},50}, \quad (\text{A7})$$

which is comparable to that of canonical GRBs. Therefore, low-luminosity GRBs have often been considered as the CR sources at ultrahigh energies [50,93].

Starburst galaxies are a subclass of star-forming galaxies. In the IR band, a significant fraction ( $\sim 5\%$ – $100\%$ ) of star-forming galaxies are claimed to be starbursts. In the local universe, however, only a few percent of the star formation occurs in starburst galaxies. The local CR luminosity density from star burst galaxies is

$$Q_{\text{cr}}^{\text{SBG}} \sim 1 \times 10^{45} \text{ erg Mpc}^{-3} \text{yr}^{-1}. \quad (\text{A8})$$

In starbursts, CRs may efficiently interact with the ambient gas and lose almost all their energies via  $pp$  interactions. Since 1/3 of the CR energy goes to pionic gamma rays, the upper limit on the gamma-ray luminosity density due to starburst galaxies is

$$Q_{\text{GeV}\gamma}^{\text{SBG}} \sim 3 \times 10^{44} \text{ erg Mpc}^{-3} \text{yr}^{-1}, \quad (\text{A9})$$

which explains  $\sim 10\%$ – $20\%$  of the EGB if a spectral index of  $s = 2.2$ , as consistent with previous studies (e.g., [94]).

Starbursts, if coexisting with AGN, could enhance the contribution to the IGRB [95].

Stars close to the center of galaxies may be tidally disrupted. Some of such tidal disruption events (TDE) show relativistic jets with an isotropic-equivalent x-ray luminosity  $L_{\text{isoy}} \sim 10^{48}$  erg s<sup>-1</sup>. Based on the Swift observation of Sw 1644 + 57, one may infer the rate density of jetting TDEs to be  $\rho_{\text{TDE}} \sim 0.03$  Gpc<sup>-3</sup> yr<sup>-1</sup> [96]. We obtain their x-ray luminosity density

$$Q_{\text{keV-MeV}\gamma}^{\text{TDE}} \sim 3 \times 10^{43} \text{ erg Mpc}^{-3} \text{ yr}^{-1} \mathcal{E}_{\text{isoy},54}, \quad (\text{A10})$$

where  $\mathcal{E}_{\text{isoy}} = L_{\text{isoy}} \Delta T$  with  $\Delta T \sim 10^6$  s the duration of TDEs [96]. This number is again comparable to the UHE CR luminosity density, and hence TDEs can also be considered as sources of UHE CRs [97,98].

## 2. Supermassive black holes

### a. Active galactic nuclei

Nonthermal x-ray emission arises from Comptonization of disc emission in thermal coronae heated via magnetic reconnections. X-ray observations give the luminosity density of AGN in the 2–10 keV band [99],

$$Q_{\text{keV}\gamma}^{\text{AGN}} \simeq 2.0 \times 10^{46} \text{ erg Mpc}^{-3} \text{ yr}^{-1}, \quad (\text{A11})$$

which is comparable to the CR luminosity density of star-forming galaxies. We note that a large part of the observed x-ray background is ascribed to unresolved and obscured AGN.

The bolometric luminosity of x rays, which is dominated by supermassive black holes with a standard accretion disc or a radiatively more efficient slim disc, is mostly of thermal origin, giving  $Q_{\text{bol}}^{\text{AGN}} \simeq 6.3 \times 10^{47}$  erg Mpc<sup>-3</sup> yr<sup>-1</sup> [99]. Recent observations indicate that quasars and Seyferts ubiquitously possess fast outflows, which carry ~10% of the bolometric luminosity [100,101]. Then, if  $\epsilon_{\text{cr}} \sim 10\%$  of the kinetic luminosity is converted into CRs via the acceleration, we may have

$$Q_{\text{cr}}^{\text{AGN}} \sim 6 \times 10^{45} \text{ erg Mpc}^{-3} \text{ yr}^{-1} \epsilon_{\text{cr},-1}, \quad (\text{A12})$$

which is comparable to Eq. (A3) within an order of magnitude.

AGN outflows driven by a central AGN are also relevant for reacceleration in circumgalactic space: CRs may further be accelerated in powerful galactic winds. As mentioned in the main text, the reacceleration in low-density regions could explain very high-energy CRs above the knee energy.

### b. Blazars

The luminosity density of blazars is estimated using *Fermi*'s gamma-ray data in the 0.1–100 GeV range. Blazars are divided into two types, BL Lac objects and

flat-spectrum radio quasars (FSRQs). The latter is also referred to as quasar-hosted blazars. They are usually more luminous and more rapidly evolving than BL Lacs. With a luminosity-dependent evolution model, the local gamma-ray luminosity of BL Lac objects is [102]

$$Q_{\text{GeV}\gamma}^{\text{BLlac}} \simeq 2.5 \times 10^{45} \text{ erg Mpc}^{-3} \text{ yr}^{-1}, \quad (\text{A13})$$

where ~50% errors in  $1\sigma$  is understood. The gamma-ray data show that BL Lacs have a weak evolution in redshift, corresponding to  $\xi_z \sim 0.8$ . The gamma-ray energy density is  $\Omega_\gamma \sim 10^{-10.0}$ , which is comparable in order of magnitude to that of the EGB. It has been suggested that BL Lacs can explain a significant fraction of the EGB. A recent analysis on the photon count distribution [64] claimed that  $86 \pm 14\%$  of the EGB are explained by blazars.

Similarly, the local gamma-ray luminosity density of FSRQs is [102]

$$Q_{\text{FSRQ}}^{\text{GeV}\gamma} \sim 2 \times 10^{44} \text{ erg Mpc}^{-3} \text{ yr}^{-1}, \quad (\text{A14})$$

with errors by a factor of 2. FSRQs show a strong redshift evolution:  $\xi_z \sim 8$ . The gamma-ray energy density of FSRQs is estimated to be  $\Omega_\gamma \sim 10^{-10.1}$ , which may also account for a significant fraction of the EGB. At present epoch, the energy densities of gamma rays from BL Lacs and FSRQs seem comparable.

### c. Misaligned radio-loud active galactic nuclei

The number density of misaligned radio-loud AGN [103,104] is  $n_{\text{RG}} \sim 10^{-5} - 10^{-4}$  Mpc<sup>-3</sup>. Radio observations allow us to estimate the kinetic luminosity of jets  $\sim 10^{44} - 10^{45}$  erg s<sup>-1</sup> [105,106], using theoretically motivated scaling relations. Assuming that  $\epsilon_{\text{cr}} \sim 10\%$  of the jet luminosity is converted to CRs, the CR luminosity density reads

$$Q_{\text{cr}}^{\text{RG}} \sim 3 \times 10^{46} \text{ erg Mpc}^{-3} \text{ yr}^{-1} \epsilon_{\text{cr},-1}, \quad (\text{A15})$$

which is comparable to or could even be larger than the CR luminosity density from star-forming galaxies. A large systematic uncertainty, however, comes from the used relationship between the radio and jet luminosities.

Radio galaxies are observed with *Fermi* in gamma rays. If we use the empirical relation, e.g.,  $L_\gamma \propto L_{5\text{GHz}}^{1.16}$ , radio galaxies make a significant contribution to the EGB [107,108]. It is found that  $\Omega_\gamma \sim 10^{-10.1}$ , however, with a large uncertainty, corresponding to

$$Q_{\text{GeV}\gamma}^{\text{RG}} \sim 4 \times 10^{44} \text{ erg Mpc}^{-3} \text{ yr}^{-1}. \quad (\text{A16})$$

It is likely that misaligned radio-loud AGN give a contribution to the EGB comparable to that of blazars. If we assume the beaming factor of AGN jets  $f_b \ll 1$ , the source number density of blazars is  $f_b$  times that of radio galaxies,

and their isotropic-equivalent luminosity is enhanced by the same factor  $f_b^{-1}$ . Thus,  $f_b$  cancels out. Their gamma ray contribution being similar to that from blazar is then naturally understood if the blazar and radio galaxies are in fact the same entity.

### 3. Hierarchical structure formation

Extragalactic CRs may also be accelerated in clusters and groups of galaxies, where the intergalactic medium is heated (e.g., [109,110]). Accretion luminosity of galaxy cluster is  $L \approx (\Omega_b/\Omega_m)GM\dot{M}/r_{\text{vir}} \simeq 0.9 \times 10^{46} \text{ erg s}^{-1} M_{15}^{1/3}$ , where  $M$  is the cluster (or group) mass and  $r_{\text{vir}}$  the virial radius. The cluster number density above  $10^{15} M_\odot$  is  $n_{\text{cl}} \sim 10^{-6} \text{ Mpc}^{-3}$ . Assuming  $\epsilon_{\text{cr}} \sim 10\%$ , the CR

luminosity density due to accretion shocks is on the order

$$Q_{\text{cr}} \sim 3 \times 10^{46} \text{ erg Mpc}^{-3} \text{ yr}^{-1} \epsilon_{\text{cr},-1}, \quad (\text{A17})$$

which is comparable to that of star-forming galaxies and radio galaxies within an order of magnitude.

As a result of hierarchical halo mergers, the kinetic energy is dissipated by shocks caused by galaxy and cluster mergers. The CR luminosity due to the halo mergers is [111],

$$Q_{\text{cr}} \sim 2 \times 10^{45} \text{ erg Mpc}^{-3} \text{ yr}^{-1} \epsilon_{\text{cr},-1}, \quad (\text{A18})$$

which is comparable to CRs in starburst galaxies.

- 
- [1] M. Fukugita and P. J. E. Peebles, *Astrophys. J.* **616**, 643 (2004).
- [2] K. Murase, M. Ahlers, and B. C. Lacki, *Phys. Rev. D* **88**, 121301 (2013).
- [3] B. Katz, E. Waxman, T. Thompson, and A. Loeb, arXiv:1311.0287.
- [4] O. Adriani *et al.* (PAMELA Collaboration), *Science* **332**, 69 (2011).
- [5] M. Aguilar *et al.* (AMS-02 Collaboration), *Phys. Rev. Lett.* **114**, 171103 (2015).
- [6] A. Aab *et al.* (Pierre Auger Collaboration), in *Proceedings of the 35th International Cosmic Ray Conference (ICRC 2017), Bexco, Busan, Korea, 2017* (2017), arXiv:1708.06592.
- [7] Pierre Auger and Telescope Array Collaborations, in *Proceedings of 35th International Cosmic Ray Conference (ICRC 2017), Bexco, Busan, Korea, 2017* (2018), arXiv:1801.01018.
- [8] M. Ackermann *et al.* (Fermi LAT Collaboration), *Astrophys. J.* **799**, 86 (2015).
- [9] M. G. Aartsen *et al.* (IceCube Collaboration), arXiv:1710.01191.
- [10] Y. S. Yoon *et al.*, *Astrophys. J.* **728**, 122 (2011).
- [11] M. Aguilar *et al.* (AMS-02 Collaboration), *Phys. Rev. Lett.* **115**, 211101 (2015).
- [12] M. J. Boschini *et al.*, *Astrophys. J.* **840**, 115 (2017).
- [13] E. C. Stone, A. C. Cummings, F. B. McDonald, B. C. Heikkila, N. Lal, and W. R. Webber, *Science* **341**, 150 (2013).
- [14] C. Corti, V. Bindi, C. Consolandi, and K. Whitman, *Astrophys. J.* **829**, 8 (2016).
- [15] M. Di Mauro, F. Donato, N. Fornengo, and A. Vittino, *J. Cosmol. Astropart. Phys.* **05** (2016) 031.
- [16] K. Blum, B. Katz, and E. Waxman, *Phys. Rev. Lett.* **111**, 211101 (2013).
- [17] O. Adriani *et al.* (PAMELA Collaboration), *Astrophys. J.* **791**, 93 (2014).
- [18] M. Aguilar *et al.* (AMS-02 Collaboration), *Phys. Rev. Lett.* **117**, 231102 (2016).
- [19] G. Giacinti, M. Kachelriess, and D. V. Semikoz, *Phys. Rev. D* **91**, 083009 (2015).
- [20] M. Aguilar *et al.* (AMS-02 Collaboration), *Phys. Rev. Lett.* **120**, 021101 (2018).
- [21] A. Neronov, D. Malyshev, and D. V. Semikoz, *Astron. Astrophys.* **606**, A22 (2017).
- [22] M. Fukugita, C. J. Hogan, and P. J. E. Peebles, *Astrophys. J.* **503**, 518 (1998).
- [23] T. Fang, J. Bullock, and M. Boylan-Kolchin, *Astrophys. J.* **762**, 20 (2013).
- [24] J. K. Werk, J. X. Prochaska, J. Tumlinson, M. S. Peeples, T. M. Tripp *et al.*, *Astrophys. J.* **792**, 8 (2014).
- [25] Y. Zheng, M. E. Putman, J. E. G. Peek, and M. R. Joung, *Astrophys. J.* **807**, 103 (2015).
- [26] T. C. Licquia and J. A. Newman, *Astrophys. J.* **806**, 96 (2015).
- [27] H. Nakanishi and Y. Sofue, *Publ. Astron. Soc. Jpn.* **68**, 5 (2016).
- [28] L. O. Drury, *Astropart. Phys.* **39**, 52 (2012).
- [29] K. Beuermann, G. Kanbach, and E. M. Berkhuijsen, *Astron. Astrophys.* **153**, 17 (1985).
- [30] A. Abramowski *et al.* (H.E.S.S. Collaboration), *Nature (London)* **531**, 476 (2016).
- [31] F. Acero *et al.* (Fermi LAT Collaboration), *Astrophys. J. Suppl. Ser.* **223**, 26 (2016).
- [32] D. Gaggero, D. Grasso, A. Marinelli, M. Taoso, and A. Urbano, *Phys. Rev. Lett.* **119**, 031101 (2017).
- [33] A. W. Strong, T. A. Porter, S. W. Digel, G. Jóhannesson, P. Martin, I. V. Moskalenko, E. J. Murphy, and E. Orlando, *Astrophys. J.* **722**, L58 (2010).
- [34] S. M. Adams, C. S. Kochanek, J. F. Beacom, M. R. Vagins, and K. Z. Stanek, *Astrophys. J.* **778**, 164 (2013).
- [35] P. Lipari, arXiv:1407.5223.
- [36] K. Blum, *J. Cosmol. Astropart. Phys.* **11** (2011) 037.
- [37] W. R. Webber and A. Soutoul, *Astrophys. J.* **506**, 335 (1998).

- [38] R. Taillet and D. Maurin, *Astron. Astrophys.* **402**, 971 (2003).
- [39] P. Madau and M. Dickinson, *Annu. Rev. Astron. Astrophys.* **52**, 415 (2014).
- [40] W. R. Webber and T. L. Villa, [arXiv:1806.02808](https://arxiv.org/abs/1806.02808).
- [41] M. L. Ahnen *et al.* (MAGIC Collaboration), *Mon. Not. R. Astron. Soc.* **472**, 2956 (2017); **476**, 2874(E) (2018).
- [42] J. G. Kirk, P. Duffy, and Y. A. Gallant, *Astron. Astrophys.* **314**, 1010 (1996).
- [43] Y. Ohira, K. Murase, and R. Yamazaki, *Astron. Astrophys.* **513**, A17 (2010).
- [44] A. R. Bell, K. M. Schure, and B. Reville, *Mon. Not. R. Astron. Soc.* **418**, 1208 (2011).
- [45] Y. Ohira, *Astrophys. J.* **758**, 97 (2012).
- [46] S. S. Cerri, D. Gaggero, A. Vittino, C. Evoli, and D. Grasso, *J. Cosmol. Astropart. Phys.* **10** (2017) 019.
- [47] F.-K. Peng, X.-Y. Wang, R.-Y. Liu, Q.-W. Tang, and J.-F. Wang, *Astrophys. J.* **821**, L20 (2016).
- [48] V. Verzi, D. Ivanov, and Y. Tsunesada, *Prog. Theor. Exp. Phys.* **12**, 12A103 (2017).
- [49] K. Murase and H. Takami, *Astrophys. J.* **690**, L14 (2009).
- [50] B. T. Zhang, K. Murase, S. S. Kimura, S. Horiuchi, and P. Mészáros, *Phys. Rev. D* **97**, 083010 (2018).
- [51] B. Katz, R. Budnik, and E. Waxman, *J. Cosmol. Astropart. Phys.* **03** (2009) 020.
- [52] G. Decerprit and D. Allard, *Astron. Astrophys.* **535**, A66 (2011).
- [53] D. Allard, *Astropart. Phys.* **39–40**, 33 (2012).
- [54] J. Heinze, D. Boncioli, M. Bustamante, and W. Winter, *Astrophys. J.* **825**, 122 (2016).
- [55] R. A. Batista, R. M. de Almeida, B. Lago, and K. Kotera, *J. Cosmol. Astropart. Phys.* **01** (2019) 002.
- [56] D. Wittkowski (Pierre Auger Collaboration), *Proc. Sci., ICRC20172018* (2018) 563.
- [57] K. Fang and K. Murase, *Nat. Phys.* **14**, 396 (2018).
- [58] H. Takami, K. Murase, S. Nagataki, and K. Sato, *Astropart. Phys.* **31**, 201 (2009).
- [59] This conclusion is unaltered if we use  $s_{\text{cr}} = 2.25\text{--}2.33$  above 3 TeV, from the CREAM experiment [10]. The CREAM data imply that spectral indices for nuclei heavier than helium can be harder,  $s_{\text{cr}} \sim 2.2$  with large errors. Their fluxes are smaller than the proton and helium fluxes, and the UHE CRs around the ankle energy is dominated by light nuclei such as protons (even though the CRs above the ankle could consist of heavier nuclei).
- [60] M. G. Aartsen *et al.* (IceCube Collaboration), *Astrophys. J.* **809**, 98 (2015).
- [61] M. Ahlers and K. Murase, *Phys. Rev. D* **90**, 023010 (2014).
- [62] K. Murase, D. Guetta, and M. Ahlers, *Phys. Rev. Lett.* **116**, 071101 (2016).
- [63] E. Waxman and J. N. Bahcall, *Phys. Rev. D* **59**, 023002 (1998).
- [64] M. Ackermann *et al.* (Fermi LAT Collaboration), *Phys. Rev. Lett.* **116**, 151105 (2016).
- [65] H.-S. Zechlin, A. Cuoco, F. Donato, N. Fornengo, and A. Vittino, *Astrophys. J. Suppl. Ser.* **225**, 18 (2016).
- [66] M. Lisanti, S. Mishra-Sharma, L. Necib, and B. R. Safdi, *Astrophys. J.* **832**, 117 (2016).
- [67] V. S. Berezinsky and A. Yu. Smirnov, *Astrophys. Space Sci.* **32**, 461 (1975).
- [68] K. Murase, J. F. Beacom, and H. Takami, *J. Cosmol. Astropart. Phys.* **08** (2012) 030.
- [69] B. C. Lacki, *Mon. Not. R. Astron. Soc.* **448**, L20 (2015).
- [70] A. Loeb and E. Waxman, *J. Cosmol. Astropart. Phys.* **05** (2006) 003.
- [71] T. A. Thompson, E. Quataert, E. Waxman, and A. Loeb, [arXiv:astro-ph/0608699](https://arxiv.org/abs/astro-ph/0608699).
- [72] K. Murase and E. Waxman, *Phys. Rev. D* **94**, 103006 (2016).
- [73] J. R. Jokipii and G. Morfill, *Astrophys. J.* **312**, 170 (1987).
- [74] H. J. Volk and V. N. Zirakashvili, *Astron. Astrophys.* **417**, 807 (2004).
- [75] T. M. Heckman, L. Armus, and G. K. Miley, *Astrophys. J. Suppl. Ser.* **74**, 833 (1990).
- [76] R. Genzel, S. Newman, T. Jones, N. M. F. Schreiber, K. Shapiro, S. Genel, S. J. Lilly, A. Renzini, L. J. Tacconi, N. Bouché *et al.*, *Astrophys. J.* **733**, 101 (2011).
- [77] S. Veilleux, G. Cecil, and J. Bland-Hawthorn, *Annu. Rev. Astron. Astrophys.* **43**, 769 (2005).
- [78] T. M. Heckman and T. A. Thompson, [arXiv:1701.09062](https://arxiv.org/abs/1701.09062).
- [79] M. Su, T. R. Slatyer, and D. P. Finkbeiner, *Astrophys. J.* **724**, 1044 (2010).
- [80] E. Sturm, E. González-Alfonso, S. Veilleux, J. Fischer, J. Graciá-Carpio, S. Hailey-Dunsheath, A. Contursi, A. Poglitsch, A. Sternberg, R. Davies *et al.*, *Astrophys. J.* **733**, L16 (2011).
- [81] T. A. Thompson, E. Quataert, E. Waxman, N. Murray, and C. L. Martin, *Astrophys. J.* **645**, 186 (2006).
- [82] D. Guetta and M. Della Valle, *Astrophys. J.* **657**, L73 (2007).
- [83] B. Abbott *et al.* (Virgo and LIGO Scientific Collaborations), *Phys. Rev. Lett.* **119**, 161101 (2017).
- [84] E. Waxman, *Phys. Rev. Lett.* **75**, 386 (1995).
- [85] M. Vietri, *Astrophys. J.* **453**, 883 (1995).
- [86] J. F. Graham and P. Schady, *Astrophys. J.* **823**, 154 (2016).
- [87] D. Wanderman and T. Piran, *Mon. Not. R. Astron. Soc.* **406**, 1944 (2010).
- [88] N. Wygoda, D. Guetta, M.-A. Mandich, and E. Waxman, *Astrophys. J.* **824**, 127 (2016).
- [89] S. Campana *et al.*, *Nature (London)* **442**, 1008 (2006).
- [90] A. M. Soderberg *et al.*, *Nature (London)* **442**, 1014 (2006).
- [91] E. Liang, B. Zhang, and Z. Dai, *Astrophys. J.* **662**, 1111 (2007).
- [92] H. Sun, B. Zhang, and Z. Li, *Astrophys. J.* **812**, 33 (2015).
- [93] K. Murase, K. Ioka, S. Nagataki, and T. Nakamura, *Astrophys. J.* **651**, L5 (2006).
- [94] M. Ackermann *et al.* (Fermi LAT Collaboration), *Astrophys. J.* **755**, 164 (2012).
- [95] I. Tamborra, S. Ando, and K. Murase, *J. Cosmol. Astropart. Phys.* **09** (2014) 043.
- [96] D. N. Burrows, J. A. Kennea, G. Ghisellini, V. Mangano, B. Zhang, K. L. Page, M. Eracleous, P. Romano, T. Sakamoto, A. D. Falcone *et al.*, *Nature (London)* **476**, 421 (2011).
- [97] G. R. Farrar and A. Gruzinov, *Astrophys. J.* **693**, 329 (2009).
- [98] G. R. Farrar and T. Piran, [arXiv:1411.0704](https://arxiv.org/abs/1411.0704).

- [99] Y. Ueda, M. Akiyama, G. Hasinger, T. Miyaji, and M. G. Watson, *Astrophys. J.* **786**, 104 (2014).
- [100] F. Tombesi, M. Cappi, J. N. Reeves, R. S. Nemmen, V. Braito, M. Gaspari, and C. S. Reynolds, *Mon. Not. R. Astron. Soc.* **430**, 1102 (2013).
- [101] F. Tombesi and M. Cappi, *Mon. Not. R. Astron. Soc.* **443**, L104 (2014).
- [102] M. Ajello, R. Romani, D. Gasparrini, M. Shaw, J. Bolmer *et al.*, *Astrophys. J.* **780**, 73 (2014).
- [103] C. J. Willott, S. Rawlings, K. M. Blundell, M. Lacy, and S. A. Eales, *Mon. Not. R. Astron. Soc.* **322**, 536 (2001).
- [104] S. van Velzen, H. Falcke, P. Schellart, N. Nierstenhoefer, and K.-H. Kampert, *Astron. Astrophys.* **544**, A18 (2012).
- [105] C. J. Willott, S. Rawlings, K. M. Blundell, and M. Lacy, *Mon. Not. R. Astron. Soc.* **309**, 1017 (1999).
- [106] K. W. Cavagnolo, B. R. McNamara, P. E. J. Nulsen, C. L. Carilli, C. Jones, and L. Birzan, *Astrophys. J.* **720**, 1066 (2010).
- [107] Y. Inoue, *Astrophys. J.* **733**, 66 (2011).
- [108] D. Hooper, T. Linden, and A. Lopez, *J. Cosmol. Astropart. Phys.* **08** (2016) 019.
- [109] H. Kang, D. Ryu, and T. W. Jones, *Astrophys. J.* **456**, 422 (1996).
- [110] K. Murase, S. Inoue, and S. Nagataki, *Astrophys. J.* **689**, L105 (2008).
- [111] C. Yuan, P. Mészáros, K. Murase, and D. Jeong, *Astrophys. J.* **857**, 50 (2018).